

# PAPER

## A Quantitative, Verifiable, and Efficacious Protocol for Spiking Solid, Granular Matrices with Radionuclidic Solutions

R. Collé and F.J. Schima

National Institute of Standards and Technology

A generalized protocol for radionuclidic spiking of solid, granular matrices (e.g., soils and sands for gamma-ray-spectrometry calibration sources in Marinelli-beaker configurations) has been devised and developed. The protocol has been found to be very quantitative (in terms of the retention of chemically stable spiking radionuclides and the recovery of the spiked matrix), verifiable (in terms of, for example, demonstrating source homogeneity or accounting for possible spike losses) and efficacious (in terms of its suitability for producing spiked sources and ability to be easily reproduced).

### Introduction

The National Institute of Standards and Technology (NIST), at the request of participating laboratories in a measurement assurance program for the nuclear power industry,<sup>1</sup> recently prepared and calibrated a spiked, mixed-radionuclide, mock "soil" source (in a 1-L Marinelli-beaker configuration) that could be used as an in-house calibration standard for gamma-ray spectrometry.<sup>2</sup> The principal objective of this work was to effect a mechanism whereby NIST could provide calibration services for other Marinelli-beaker sources that might be prepared and supplied by other laboratories (with the necessary provisos that these sources are in the same geometry, use the same matrix, and contain the same radionuclides). A secondary objective was to devise and develop a suitable spiking and preparation scheme that could be readily invoked by any other laboratories. The principal criteria for the latter objective were that any devised protocol must be eas-

ily reproducible (using readily available stock materials), quantitatively reliable (in terms of being able to relate gamma-ray emission-rate concentrations for a spiking solution to the emission rates for the mock "soil" in the Marinelli-beaker calibration source), and verifiable (in terms of source homogeneity, accounting for possible losses of spiking radionuclides, etc.).

By consensus and specification of the requesting laboratories, the Marinelli-beaker mock "soil" calibration source was to consist of an Ottawa sand matrix in a GA-MA "130G" (nominal 1 L) polyethylene standard configuration beaker, that would be spiked with the usual mix (<sup>109</sup>Cd, <sup>57</sup>Co, <sup>139</sup>Ce, <sup>203</sup>Hg, <sup>113</sup>Sn, <sup>85</sup>Sr, <sup>137</sup>Cs, <sup>88</sup>Y, and <sup>60</sup>Co) present in the original NIST mixed-radionuclide gamma-ray emission-rate standard<sup>3</sup> and adopted by other secondary calibration laboratories and commercial vendors of radioactivity standards. It was decided to also include

$^{241}\text{Am}$  in the spiking to extend the range of the calibration source to lower energies.

This paper describes the generalized protocol that was developed to prepare the Marinelli-beaker mock "soil" calibration source. It was used for two different mock "soil" matrices; a standard Ottawa sand (designated OS), and a granular NaCl (designated GS). The latter was pursued for reasons outlined below. One Marinelli-beaker source of each (along with matched blanks) were prepared. In addition to the high-resolution photonic-emission-rate calibration on the final OS1 standard, many other evaluations (such as for matrix recoveries, spiking losses, source homogeneity, etc.) were also performed.

## Spectrometry and calibration standard considerations

The use of Marinelli beakers for gamma-ray spectrometry of large-volume samples (typically for soils, sludges, or waters), such as for monitoring or surveillance around nuclear power facilities, is well known. Marinelli beakers that are designed to closely fit over and envelop the endcaps of detectors tend to optimize geometrical detection efficiencies. Their standardized dimensional specifications (in various sizes)<sup>4</sup> not only ensure a standard detection geometry, but also provide crudely comparable self-absorption in bulk samples of similar composition.

Marinelli-beaker calibrations require detection-efficiency determinations (for a given beaker-detector geometry) with bulk standard sources having known radionuclidic content. Any such source should reasonably simulate the "self-absorption" characteristics of typical samples that are to be assayed. That is, they should have reasonably matched photon absorption, attenuation, and scattering properties; that in turn requires similar atomic constituents, similar concentrations of these constituents, and similar bulk densities. This requirement is formidable considering all possibilities of solid matrices that are of assaying interest.

An additional consideration is the choice of radionuclides to be used in the standard for calibration purposes. Ideally, the source would contain

every possible radionuclide that is to be measured. This is hopelessly impractical inasmuch as it would result in requiring a horrendous complex of radionuclides, many of which may not exist as standards with primary calibrations and may have half-lives that are too short to serve as useful calibration sources. The alternative, of course, is to use select radionuclides for the calibration, and to develop a conventional detection-efficiency versus photon-energy calibration curve that includes self-absorption corrections. This too only works in the ideal if one can appropriately select (and find) a sufficient number of certified radionuclidic standards having only mono-energetic gamma-ray emissions<sup>5,6</sup> that thereby avoid the often large coincident-photon-summing losses attendant with many coincident gamma-ray standards (like  $^{133}\text{Ba}$ ,  $^{60}\text{Co}$ ,  $^{88}\text{Y}$ ). These coincidence-summing problems in Marinelli-beaker configurations (and the limiting energy range of readily-available, coincident-free gamma-ray standards) have been addressed, in a very practical way, by McFarland.<sup>5</sup>

Solid matrix inhomogeneity in Marinelli beakers is another consideration in terms of its effects on geometrical (subtended solid angle) efficiency and self-absorption differences.<sup>7</sup> These effects may also be temporal; that can occur, for example, with the settling (sedimentation) of matrix particles having differing sizes and densities. Homogeneity requirements for Marinelli-beaker calibration sources are nowhere near as stringent as those required for spiked samples used for wet radiochemical assay procedures.<sup>8,9</sup> For the latter, any given aliquant of the standard (compared to any other aliquant) must be homogeneous (to the desired accuracy of the assay) in the smallest aliquant used for the assay (typically 10 g or less). In contradistinction, gamma-ray spectrometry of bulk samples is largely a less discriminating measurement that has the ability to average over many small differences in the radionuclidic distribution in the source. Nevertheless, any systematic (spatially structured) inhomogeneities will result in an inherent error. This might occur, for example, if one particular radionuclide is

preferentially associated (by containment or adsorption) with the most dense matrix particles that gradually settle to the bottom of the beaker.

Numerically-calculated corrections for geometrical efficiency and self-absorption effects for gamma rays in different (detection geometry) volumes, and for coincident-photon-summing corrections in these same geometries are well within present-day computational capabilities (cf., Debertin and Helmer<sup>10</sup> and references therein). Whether these capabilities, particularly for volume-dependent coincident-gamma-ray summing loss calculations,<sup>11</sup> can be readily translated into practical algorithms for routine laboratory use is dependent upon many factors. Carefully prepared and well-characterized spiked sources with known radionuclidic content (and having both substantial self-absorption and coincident-photon-summing losses) in Marinelli-beaker geometries, such as those described herein, could be valuable in evaluating or validating the adequacy of such algorithms.

## Matrix selection considerations

The original selection of Ottawa sand for the mock "soil" matrix was initially considered to be a possibly poor to mediocre choice. Its principal advantage is that it is readily available (from many chemical supply vendors) with well-characterized physical properties. It is granular and can be obtained (as 20-30 mesh) with a fairly narrow particle-size distribution. Particle-size measurements by this laboratory have demonstrated that over 98% of the particles (by mass) are in a range 0.59 mm to 0.84 mm (Appendix). Bulk density, grain density, and volume packing determinations were also made. Obviously, this matrix might not appropriately simulate finer mesh soils, e.g., 200 to 325 mesh (0.075 to 0.045 mm), and soils of different densities and other compositions.

Our principal initial concern in using Ottawa sand was that we thought it may have a low adsorption capability. The concern would be that the spiking radionuclides may not easily adhere to the sand par-

ticles and/or may be lost in handling (e.g., with agitation during blending) or in usage (e.g., with settling in the Marinelli beaker). Hence, an alternative granular NaCl (salt) matrix was also pursued, mainly because of the above concern with Ottawa sand. A similar kind of spiked NaCl matrix has been reported to be in use as a mock "soil" calibration source at the TVA laboratory.<sup>12</sup> We reasoned that in the case of the granular salt, the spiking would not rely on physical or Van der Waals' adsorption of the spiked radionuclides on particles of silica or mixed silicates. Rather, it relies on actual chemical adsorption (chemisorption) that results in firm chemical bonds between the spiking radionuclides and matrix crystals. When the spiking solution is deposited as fine droplets onto the sodium chloride granules, some portion of the crystals dissolve; but the deposited solution immediately re-crystallizes as mixed salts of the spiking radionuclide and NaCl (since the dissolved solution is super-saturated). The Appendix also summarizes some properties of the granular-salt matrix.

In retrospect, it is now evident that Ottawa sand is sufficiently adsorptive to adequately serve as the spiked matrix. During the course of this project however, we also learned what criteria one might use to select more adsorptive matrices of either real soils or stone aggregates. These might include: soils containing clay minerals that show a marked adsorptive capacity, and other pulverized, granular stone aggregates that are known to have greater "strength", i.e. better adsorption properties. The "strength" of a cement prepared from a given aggregate (usually defined in terms of some specific type of stress test) can be used as a crude guide or relative measure of the adsorptive capability of the aggregate. One might therefore expect a pulverized limestone to be worse than Ottawa sand, and certain Georgian marbles to be better, for examples.

## Spiking protocol

The scheme used to prepare the mock "soil" Marinelli-beaker calibration source OS1 is outlined in Figure 1. Although many of the features (e.g.,

the initial solution handlings and assays to arrive at master spiking solution M1) are specific to this preparation, the figure is primarily intended to illustrate the principal features (and advantages) of the devised protocol. The scheme can be readily adopted

with necessary minor modifications for similar or related source preparation applications. A detailed descriptive summary of this preparation, however, should serve as a sufficient demonstrative example of the application of the protocol. The example

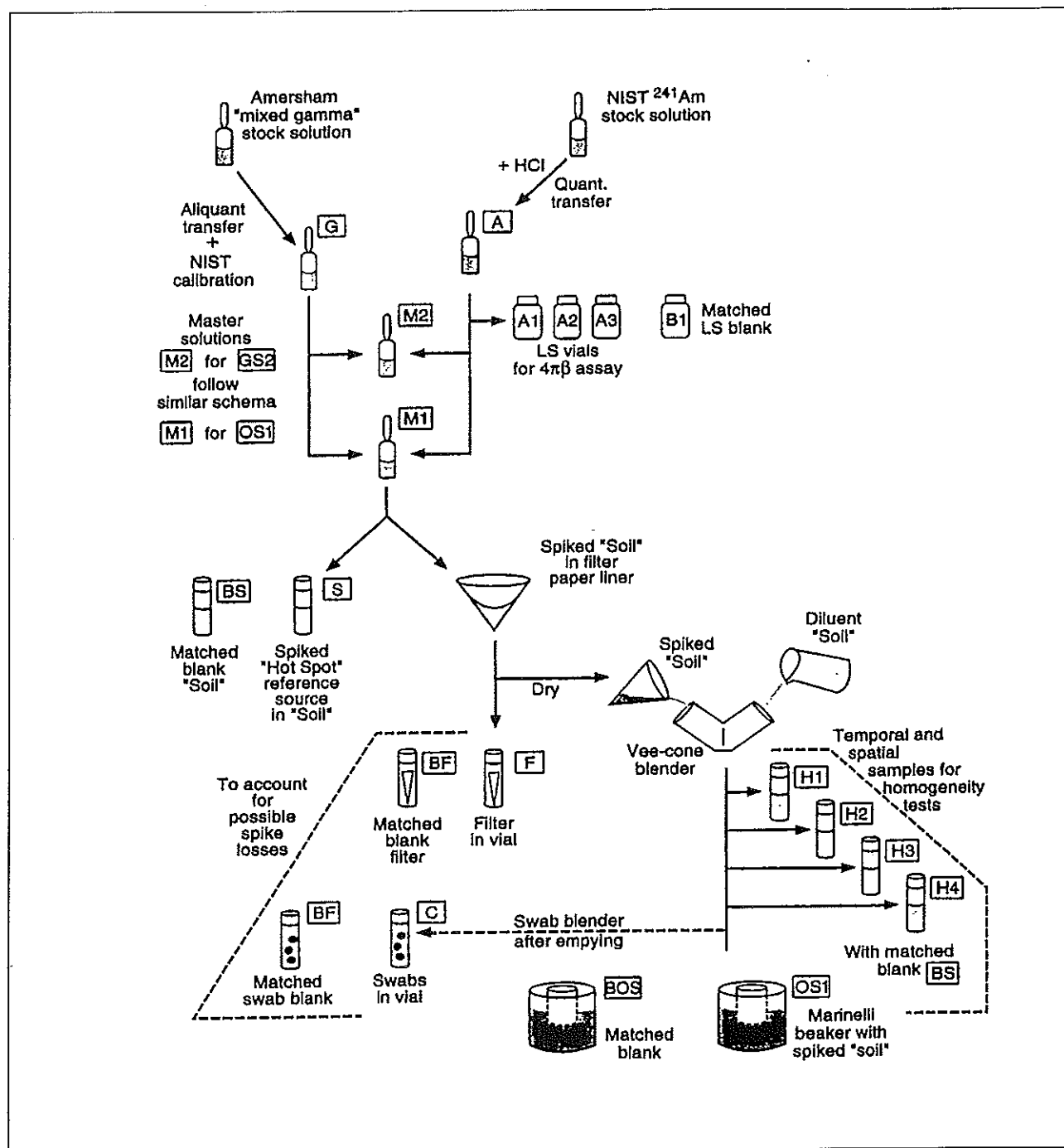


Figure 1. Schema for the spiking and preparation of the mock "soil" (Ottawa sand) Marinelli-beaker calibration standard.

may prove useful in demonstrating the attainable levels of precision that can be obtained through careful and controlled laboratory practices.

### Stock and master spiking solutions

The master spiking solutions (labeled solutions M1 and M2 in Figure 1) that were used to prepare the Marinelli-beaker sources OS1 and GS2 were prepared by combining gravimetrically-determined aliquants of stock solutions G and A in 5-mL ampoules. The latter solution, as noted previously, was used to incorporate  $^{241}\text{Am}$  into the spiked source.

Solution G was a mixed-radionuclide gamma-ray reference source originally obtained from Amersham. The solution was in a flame-sealed 5-mL ampoule, and contained the usual mix of nine radionuclides (given previously) in  $4 \text{ mol} \cdot \text{L}^{-1} \text{ HCl}$  ( $1.067 \text{ g} \cdot \text{mL}^{-1}$  at  $20^\circ \text{C}$ ). The original solution was certified by Amersham for  $\gamma \cdot \text{s}^{-1} \cdot \text{g}^{-1}$  of solution for 11 photons. The contents of the original solution was gravimetrically transferred to a new NIST standard 5-mL ampoule, and was re-assayed by NIST for the emission-rate concentration for each of the 11 photons. The NIST re-assays were performed with cooled, high-purity Ge detectors having well-established efficiency curves in a standard geometry for the NIST 5-mL ampoule. The relative standard uncertainties on each emission-rate concentration, as obtained from the NIST re-assay, ranged from 0.33 to 0.82%. Comparisons between the original Amersham certified values and those obtained by NIST (with decay) indicated agreement to better than 0.1 to 0.2% in general for each of the 11 photons (and was 0.5% in a worst case for the 88-keV  $^{109}\text{Cd}$  gamma ray).

Solution A was derived from a stock of NIST  $^{241}\text{Am}$  in a 2-mL ampoule that contained a nominally known total activity in a small volume (roughly 0.2 mL) of  $1 \text{ mol} \cdot \text{L}^{-1} \text{ HCl}$ . The contents of the original ampoule was transferred with rinsings to a new 5-mL ampoule (labeled A). The  $^{241}\text{Am}$  activity concentration of ampoule A was assayed by  $4\pi\Omega$  liquid scintillation (LS) spectrometry, and was found

to be  $2348 \text{ Bq} \cdot \text{g}^{-1} \pm 7 \text{ Bq} \cdot \text{g}^{-1}$  as of 1200 EST 21 September 1994. The LS assay was based on 12 replicate measurements on each of three LS samples (and matched blanks for background subtraction) that were intermittently performed over the course of eight days. The cited uncertainty corresponds to a combined standard uncertainty. Detailed descriptions of the metrological practices of the NIST Radioactivity Group for the assay of alpha-particle emitters (like  $^{241}\text{Am}$ ) by LS spectrometry have been given by Collé, et al.<sup>13</sup>

The gravimetrically-determined aliquants of solutions G and A in M1 and M2 were based on "dispensed masses" obtained from differences in masses between dispensings with an aspirating pycnometer. These mass differences were also independently confirmed by the "contained masses" obtained from mass differences in the ampoules before and after dispensing. Relative differences between the dispensed and contained masses (that utilize very different internal balance weights) were less than 0.05% in all cases.

Solution ampoules G and A, prior to their use in preparing master solutions M1 and M2, were measured in a NaI(Tl) well counter to obtain relative gross gamma-ray emission rates. These rates could be subsequently compared to the results on similar measurements on M1 and M2 to independently verify the gravimetric determinations. The relative gross rates were based on integrating the full-energy NaI(Tl) spectra from approximately 20 keV to 3400 keV which included all of the  $^{241}\text{Am}$  to  $^{88}\text{Y}$  photopeaks as well as sum peaks. With this, the gravimetric combinations to prepare master solutions M1 and M2 could be independently verified from the constituent masses [ $m_{\text{A(M1)}}$ ,  $m_{\text{G(M1)}}$ ,  $m_{\text{A(M2)}}$ , and  $m_{\text{G(M2)}}$ ] and the relative gross gamma-ray emission rates  $R_{\text{G}}$  and  $R_{\text{A}}$  for solutions G and A (above). The overall agreement between directly measured rates  $R_{\text{M1}}$  and  $R_{\text{M2}}$  on solutions M1 and M2 and that obtained from the predicted weighted combinations of the rates of  $R_{\text{G}}$  and  $R_{\text{A}}$  on solutions G and A;

i.e.,

$$R_{M1} = (m_{A(M1)} R_A + m_{G(M1)} R_G) / (m_{A(M1)} + m_{G(M1)}), \text{ and}$$

$$R_{M2} = (m_{A(M2)} R_A + m_{G(M2)} R_G) / (m_{A(M2)} + m_{G(M2)})$$

were 0.092 % and 0.043 %, respectively. Similar relationships between the masses and gross gamma-emission rates could be used to verify, for example, the mass ratio of solution M1 to M2 as well as other corresponding mass pairs. Overall, the relative emission rate verifications indicated mass agreements to typically better than 0.05%, and 0.18% in a worst case.

### Schema, sequentially

For the spiking, as a first step, about 230 g of the Ottawa sand were added to a large (28-cm diam.) vee-cone filter paper that was contained in a specially-fabricated, light-weight filter holder (that permitted direct mass measurements of the holder, filter, sand, and spiking solution). Pretreatment (washing and grading) of the sand is described in the Appendix. The mass of added sand was determined gravimetrically, with replication from both a contained and dispensed sand mass. The two mass measurements agreed to within 0.004%. Containment of the mock "soil" matrix in the filter paper liner was used to evaluate any loss of spiking solution (by direct subsequent gamma-ray spectrometry of the filter). This aspect is unique in comparison to other published methods<sup>8,9</sup> used for spiking in which subsequent (sometimes heroic) efforts are normally required to assay the spiking apparatus for any residual activity.

For the second step, about 4.2 g of solution M1 was added dropwise and dispersed over the surface of the sand (contained in the filter). Care was exercised to avoid adding the solution to areas near the edges of the sand where it could percolate through the thin sand layer to the filter. The mass of added solution M1 was also determined gravimetrically from both dispensed and contained masses. The difference in this case was less than 0.002%.

The wetted sand was then allowed to slowly dry in air under a low-intensity infrared heat lamp at a temperature <60° C.

A spiked "hot spot" reference source (labeled S in Figure 1; with matched blank BS) was also prepared at the time of addition of M1 to the sand. It had a well-known (gravimetrically determined) quantity of the master spiking solution (M1) that was added to about 30 g of sand contained in a 2-cm diameter by 9-cm high, thin-walled plastic vial. It would be used for comparative measurements with later spiked samples (see following). This sample was mixed, but was not rigorously homogeneous; and small differences in relative measurements naturally arose because of this.

As a third step, the dried spiked sand matrix was quantitatively transferred to and diluted with additional sand within the 4-L (polished stainless steel) shell of a vee-cone blender (to form a total sand mass of about 1.85 kg). The masses of the transferred spiked sand and diluent sand were again carefully determined from dispensed and contained mass differences. The overall uncertainty in the total sand mass was estimated to be less than 0.1% (combined standard uncertainty).

The filter-paper liner after emptying was collected for subsequent assay for any residual activity. The final mass of the filter after spiking was also compared to its initial tare mass. The masses were identical to within the measurement precision ( $\pm 0.05\%$ ) thus indicating that no substantial quantities of minute sand particles were retained by the filter.

For the fourth step, the diluted, spiked matrix was then blended in a high-efficiency vee-cone blender (Patterson-Kelley Blendmaster) for 400 minutes. Four homogeneity aliquants (each of approximately 30 g) were collected by sampling from the blender after varying blending times (40 min to 400 min). The samples, obviously, could also provide a measure of spatial homogeneity. The sample extractions were performed carefully and the masses of the aliquants were determined to provide a complete accounting of the total sand mass. The four extracted aliquants were not returned to the blender, but

could have been had they exhibited serious inhomogeneities. These homogeneity samples (H1 through H4 in Figure 1), beside being compared on a relative basis by gamma-ray spectrometry, could also be assayed (semi-quantitatively) with respect to reference source S that had the same source geometry (i.e., in the same 2-cm-diameter by 9-cm-high plastic vials).

After blending, the total remaining spiked sand mass (1.72 kg) was quantitatively transferred (with mass determinations) to the Marinelli beaker. The beaker after filling and capping was sealed with a mastic tape.

A final step in the spiking protocol consisted of thoroughly swabbing all interior surfaces of the blender (at varying stages of dismantling) with pre-moistened swabs containing a dilute acidic EDTA-2 (ethylenediaminetetracetate) solution, and collecting the swabs for determinations of any residual activity.

### Principal features

The principal features of the protocol are: (i) that the filter-paper liner allowed for a direct evaluation of any possible loss of the spiking solution; (ii) that the "hot spot" reference source S could be used as a "standard" for semi-quantitative assays of the filter paper sample F, homogeneity samples H1 through H4, and blender swab samples C; (iii) that homogeneity could be checked both with spatial aliquants of the spiked matrix and temporally as a function of blending time; (iv) that all transfers of solutions and matrices were gravimetrically determined (usually with independent mass verifications) and provided a complete accounting of material balances; (v) that the blender was the sole piece of spiking apparatus that had to be "swiped" for assessing a possible spike loss; and (vi) that all samples (as noted in Figure 1) had matched blank counting sources.

## Evaluations and discussion

Standard OS1 on sealing consisted of 1715.9006 g of Ottawa sand that had been spiked with 3.938335 g of solution M1. The corresponding blank BOS contained 1725.6542 g of sand. Assuming a bulk density of  $1.72 \text{ g} \cdot \text{cm}^{-3}$  (Appendix), the volumes of the two sources are 0.998 L and 1.003 L, respectively. These are about 83% of the total interior volume of the beakers. The total contained beaker volumes were found to be  $1211 \text{ cm}^3 \pm 5 \text{ cm}^3$  (at  $22^\circ \text{C}$ ) where the cited uncertainty is a combined standard uncertainty. This volume measurement was based on replicate gravimetric determinations using high-purity water of known density at given temperatures for three beakers with three-point extrapolations to total capped volume.

### Matrix recovery

Standard OS1 was obtained by spiking approximately 230 g of sand with 4.238052 g of solution M1 that after drying was combined with diluent sand to form a total spiked Ottawa sand mass of 1846.4848 g. The total mass of Ottawa sand recovered after all operations was 1846.4619 g, that corresponds to an unaccounted-for-sand loss of 0.0229 g or a recovery of 99.999% of the total sand used. One may appreciatively note, that if one assumes a grain density of 0.00068 grams per grain (Appendix), then the unaccounted-for-sand loss corresponds to about 34 grains of sand lost out of 2.72 million!

### Calculated emission rates for OS1

Based on the gravimetrically-determined spiking and matrix dilution, and on the previously determined emission rates for solutions G and A that were used

PROTOCOL FOR SPIKING SOLID GRANULAR MATRICES WITH RADIONUCLIDIC SOLUTIONS  
COLLE AND SCHIMA

| radionuclide      | $\gamma$ -ray energy<br>(keV) | NIST<br>emission rate for<br>( $\gamma \text{ s}^{-1}$ ) <sup>a</sup> | relative standard<br>uncertainty<br>(%) |
|-------------------|-------------------------------|---|---|
| <sup>241</sup> Am | 59.537                        | 1442.2  | 0.89                                    |
| <sup>109</sup> Cd | 88.0341                       | 1126.4  | 0.59                                    |
| <sup>57</sup> Co  | 122.0641                      | 908.9   | 0.68                                    |
| <sup>139</sup> Ce | 165.857                       | 744.1   | 0.45                                    |
| <sup>203</sup> Hg | 279.1967                      | 444.0 <sup>b</sup>  | 1.16                                    |
| <sup>113</sup> Sn | 391.702                       | 1774.7  | 0.71                                    |
| <sup>85</sup> Sr  | 514.0076                      | 1683.6  | 0.67                                    |
| <sup>137</sup> Cs | 661.66                        | 5404.1  | 0.39                                    |
| <sup>88</sup> Y   | 898.042                       | 5201.0  | 0.53                                    |
| <sup>60</sup> Co  | 1173.238                      | 6989.6  | 0.34                                    |
| <sup>60</sup> Co  | 1332.502                      | 7014.4  | 0.34                                    |
| <sup>88</sup> Y   | 1836.063                      | 5436.9  | 0.54                                    |

<sup>a</sup>The emission rates are as of 1200 EST, 1 October 1994.  
<sup>b</sup>Spiking of <sup>203</sup>Hg was demonstrated to be nonquantitative because of its chemical instability out of solution.

Table 1. Gravimetrically-determined spiking of mixed gamma-ray standard OS1.

to prepare solution M1, the total emission rates for OS1 (as of the calibration reference time 1200 EST, 1 October 1994) were calculated and are given in Table 1.

### Spike losses

Other than a detected spike loss for <sup>203</sup>Hg, there was no evidence for any other radionuclidic losses in the spiking procedure. The <sup>203</sup>Hg loss is not nec-

essarily surprising since mercury is chemically unstable when it is out of solution and dried. The spike loss for <sup>203</sup>Hg is believed to have principally occurred during the blending process and not during wetting of the sand matrix — insofar as the spiking filter (Figure 1) contained no detectable activities. Of course, this does not necessarily exclude the possibility that the mercury might have been lost through volatilization during the initial drying process. Such

| sample | obtained from                   | fraction of M1 spike |
|--------|---------------------------------|----------------------|
| F-OS   | filter liner                    | <0.00001             |
| C2-OS  | initial blender swabs           | 0.00012              |
| C-OS   | blender swabs after dismantling | 0.0036               |

Table 2. Spike-loss results based on NaI(Tl) gross gamma-ray measurements (over the full-energy spectra) with normalization to the "hot spot" reference spike.



volatilization losses would not have been detected by analyses of the filter. Table 2 illustrates the results of detected losses from three spike-loss samples.

Based on low-resolution NaI(Tl) spectrometry with a well counter, initial spiking losses (for total gross gamma-ray activity) appeared to be less than 0.02%. This estimate was based on NaI(Tl) spectra analyses of spike-loss samples (C2-OS in Table 2) obtained from swabbing the entire interior surface of the vee-cone blender after all the spiked OS was removed. Subsequent samples (C-OS in Table 2) obtained from the seals and axle shafts of the blender after the blender was disassembled exhibited a total spike loss of roughly 0.36%. Firstly, this percentage could not be accounted for by losses of the OS. Its value was larger than the total unaccounted for loss of OS mass used in the spiking, blending and preparation processes. As noted above, the overall recovery of the OS mass used was 99.999% (23 mg lost out of over 1846 g). This finding suggests that at least part of the spike loss was not associated with unrecovered sand. It seems quite probable that the loss occurred during the blending because of detachment or volatilization of the radionuclides from the OS matrix particles. Secondly, NaI(Tl) spectral examinations of the spike-loss samples strongly demonstrated that the spiking radionuclides were present in different ratios (or fractionated differently) in the loss samples (Table 2) than in the OS samples.<sup>2</sup> It was most evident for <sup>203</sup>Hg. The location of the largest spike losses in the most inaccessible parts of the blender suggest that the radionuclides were lost as gaseous or very fine particulate matter. This apparent preferential loss of <sup>203</sup>Hg in the spiking was confirmed by high-resolution gamma-ray spectrometry on the spike-loss samples, as well as inferentially from measurements on the homogeneity samples and in the beaker calibration measurements themselves (see subsequent discussions).

As indicated previously, the nonquantitative spiking of <sup>203</sup>Hg perhaps should not be surprising since such source preparation problems frequently arise out of the volatility of many mercury compounds.

It has been demonstrated that the losses are such that <sup>203</sup>Hg can not be certified in the calibration of OS1. The use of any other mock "soil" matrix (such as the prepared GS2 source) may not resolve the problem since the mercury loss is likely to occur during any drying process, irrespective of the matrix used. A nearly comparable loss was found in GS2. One could of course envisage a modification of the preparation procedure by drying the spike in an atmosphere of hydrogen sulfide to precipitate HgS. But then, it is not apparent why the precipitated HgS would necessarily adsorb or adhere to the matrix grains, and would likely "shake off" the matrix during blending. No other such radionuclide fractionation problems or losses were found for any other radionuclides in the mix.

### Homogeneity

During blending, four homogeneity samples were collected at different blending times. These are given in Table 3.

Based on low-resolution NaI(Tl) spectrometry with a well counter, four homogeneity samples (collected after 40 to 400 minutes of blending) showed that the OS blend was homogeneous, both temporally and spatially, to within a few percent. This estimate was based on the total gross gamma-ray activity in the samples that was obtained from integrating the full-energy NaI(Tl) spectra. Crude analyses of the photopeaks for the individual radionuclides

| sample | mass of sample<br>(g) | blending time<br>(min) |
|--------|-----------------------|------------------------|
| H1-OS  | 33.6888               | 40                     |
| H2-OS  | 32.5688               | 120                    |
| H3-OS  | 33.3162               | 244                    |
| H4-OS  | 30.9877               | 400                    |

Table 3. Homogeneity samples for preparation of OS1.

in the homogeneity samples demonstrated that there were no substantial fractionation of the radionuclides in the samples, excepting that for  $^{203}\text{Hg}$ . These NaI(Tl) results were, of course, at best only semi-quantitative. The relative mean gross gamma-ray activity in the four homogeneity samples was, however, also in agreement to within about 0.5% with that expected from the total M1 solution mass spiked in the total OS mass.

Figure 2 gives the results of these gross gamma-ray activity measurements on the samples. The "homogeneity measure" given in the figure corresponds to the mass ratio M1/OS. This was obtained by normalizing the NaI(Tl) counting rate concentrations to that obtained from a known aliquant of M1 in reference source S (the "hot spot" spike — Figure 1). The displayed results are normalized values from four determinations obtained by integrating the full-energy NaI(Tl) spectra. The dotted line in Figure 2 is the gravimetrically determined M1/OS mass ratio.

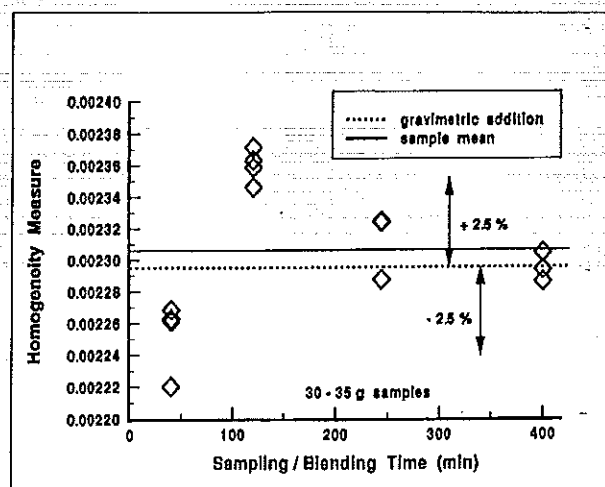


Figure 2. Evaluation of homogeneity between four aliquants of the spiked Ottawa sand (sampled after varying blending times) in terms of a "homogeneity measure" (see text) obtained from low-resolution NaI(Tl) gamma-ray spectrometry.

High-resolution gamma-ray spectrometry on the homogeneity samples of Table 3 were also performed to evaluate homogeneity for specific radionuclides. Some of the results of these measurements are given

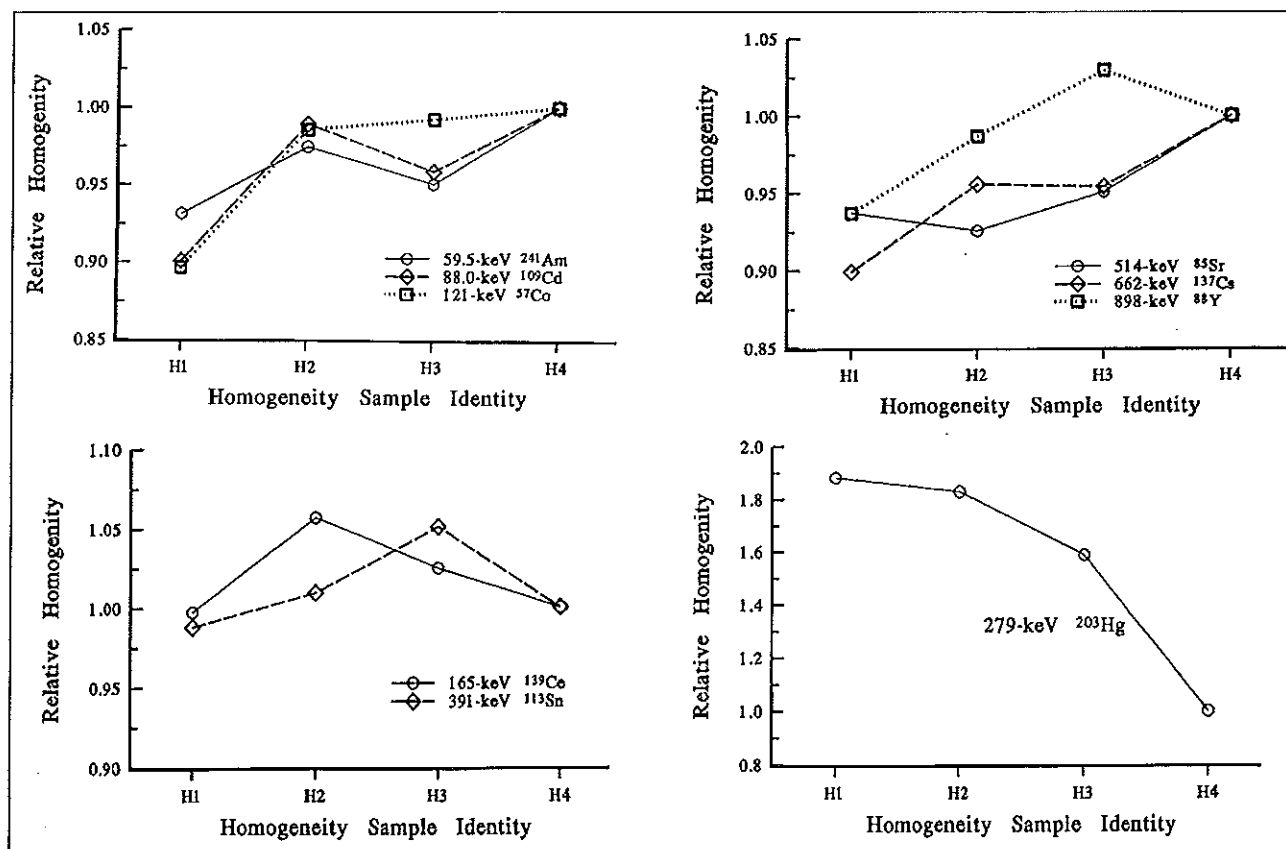


Figure 3. Relative homogeneity of the individual radionuclides in four aliquants of the spiked Ottawa sand, taken as a function of blending time (40 min to 400 min), and as measured with the high-resolution NIST "X" detector.

| radionuclide      | $\gamma$ -ray energy<br>(keV) | mean<br>relative homogeneity | standard<br>deviation |
|-------------------|-------------------------------|------------------------------|-----------------------|
| <sup>241</sup> Am | 59.537                        | 0.975                        | 0.025                 |
| <sup>109</sup> Cd | 88.0341                       | 0.983                        | 0.021                 |
| <sup>57</sup> Co  | 122.0641                      | 0.993                        | 0.007                 |
| <sup>139</sup> Ce | 165.857                       | 1.027                        | 0.028                 |
| <sup>203</sup> Hg | 279.1967                      | [1.47]                       | [0.43]                |
| <sup>113</sup> Sn | 391.702                       | 1.020                        | 0.027                 |
| <sup>85</sup> Sr  | 514.0076                      | 0.959                        | 0.038                 |
| <sup>137</sup> Cs | 661.66                        | 0.970                        | 0.026                 |
| <sup>88</sup> Y   | 898.042                       | 1.005                        | 0.022                 |

Table 4. Relative homogeneity in samples H2, H3, and H4 for the individual radionuclides as obtained with the NIST "X" detector.

in Figure 3. These results were obtained with the NIST "X" detector (an n-type intrinsic Ge with a 1-mil Be window and having an equivalent 9.9% NaI efficiency). The results of Figure 3 are normalized to the observed emission rates obtained for sample H4 (after 400 min of blending). As shown, the emission rate for sample H1 (after 40 min of blending) is almost always invariably lower than the next three samples, suggesting that perhaps an hour or so of blending is required to achieve reasonable homogeneity. The results for <sup>203</sup>Hg are dramatic and show the progressive loss of mercury over the entire blending time. Between sample H1 and H4, the <sup>203</sup>Hg loss is nearly a factor of two—despite that most of the <sup>203</sup>Hg was probably lost prior to the H1 sampling. On consideration of just the last three samples for every radionuclide, the mean relative homogeneity is typically within  $\pm 2$  or 3% of unity (excepting that for <sup>203</sup>Hg) with relative standard deviations of comparable magnitude (Table 4).

### Calibration

The standard OS1 was calibrated on the high-resolution NIST "T" detector that is a p-type intrinsic

Ge having an equivalent efficiency of 14.5% of NaI. A summary of the calibration factors for each principal photon is given in Table 5. The calibration factors are a virtual "apparent efficiency" in that they are the observed counting rates from the source for each photon divided by their respective gravimetrically-determined emission rates (Table 1). The calibration factors do not include any corrections, such as for source self-absorption or coincident-photon summing losses. Figure 4 illustrates these calibration factor data in terms of a conventional "efficiency curve". The anomalous value for <sup>203</sup>Hg clearly demonstrates the large spike loss for this radionuclide.

### Conclusions

The spiking and preparation scheme that was developed for this work was demonstrated to be very quantitative, verifiable, and efficacious. It provides a very good quantitative "handle" on the entire process; has sufficient provisions for verifying possible spiking losses and assuring source homogeneity; and "works" for the intended purpose.

The Marinelli-beaker source OS1 also appears to have "worked" in the sense that the Ottawa sand was sufficiently adsorptive and that the spiking radionuclides, excepting  $^{203}\text{Hg}$ , were quantitatively transferred from the spiking master solution M1 to the sand to better than 99.5%. Source homogeneity as determined from measurements on aliquants (30 g samples out of 1850 g of sand) was demonstrated to be within a few percent that is more than adequate for gamma-ray spectrometry in a Marinelli-beaker configuration.

The calibration obtained in this work will presently allow NIST to provide calibration services for other Marinelli-beaker sources, provided that these sources are in the same geometry, use the same Ottawa sand matrix, and contain the same radionuclides.

## Appendix: Densities, particle-size distributions, and volume packing considerations for the mock "soil" matrices

### Standard Ottawa sand (OS)

Two lots of 20-30 mesh standard Ottawa sand, obtained from Fisher Chemical were examined. As a pretreatment, to remove very fine silica dust, the sand was washed with distilled water on a 325-mesh (0.045 mm) sieve and dried under an infrared heat lamp.

The bulk density was found to be  $1.721 \text{ g} \cdot \text{cm}^{-3} \pm 0.006 \text{ g} \cdot \text{cm}^{-3}$  (one can adopt  $1.72 \text{ g} \cdot \text{cm}^{-3} \pm 0.01 \text{ g} \cdot \text{cm}^{-3}$ ) where the cited uncertainty is a standard deviation with  $\nu = 9$  degrees of freedom for 10 independent mass determinations (with both lots) in calibrated volumes of 500 and 1000  $\text{cm}^3$ . The density largely depends on extent of granular packing (that in turn determines volume of a given mass). The density given was that obtained with moderate tapping and settling. Loosely packed density can be as low as  $1.3 \text{ g} \cdot \text{cm}^{-3}$ ; and extreme packing (under pressure) as high as  $1.76 \text{ g} \cdot \text{cm}^{-3}$ . Packing in the Marinelli beaker is believed to correspond

closely to the  $(1.72 \pm 0.01) \text{ g} \cdot \text{cm}^{-3}$  density.

Gravimetric determinations of particle-size distributions for the washed sand were performed by screening through standard mesh screens and subsequent weighings of the fraction of sand retained on each screen. The particle-size distribution may be characterized as being normally distributed (very roughly) with a mean particle diameter of  $\mu = 0.7 \text{ mm}$  and standard deviation of  $\sigma = 0.1 \text{ mm}$ . Derivation of this characterization follows. Figure A1 gives the particle-size distribution for the mass fraction of particles between various mesh-size sieves. Particles below 0.045 mm are excluded because they were removed by washing. No substantial differences between samples from two lots were observed. Over 98% of the mass have mean diameters between 0.59 mm and 0.84 mm. Figure A2 gives the distribution for the number fraction of particles that was calculated from the data of Figure A1 on the assumptions that the grain density of all particles is constant and independent of grain size and that the particles are spherical (or at least that the volume of the particles is proportional to the cube of the mean particle diameter). In terms of number fraction there is an enhancement in smaller particles. Figure A3 shows a theoretically modeled particle-size distribution (based on the data of Figure A2) obtained from assuming that the particle diameters are a truncated normal distribution. This distribution can be described in terms of parameters  $\mu = 0.700 \text{ mm}$  and  $\sigma = 0.097$ . The slight discontinuities in the calculated distribution of Figure A3 are merely the result of numerical imprecision in the calculations.

The grain density was approximated to be roughly 0.00069 gram per average grain. This corresponds to  $3.6 \text{ g} \cdot \text{cm}^{-3}$  assuming a spherical mean particle diameter of 0.7 mm—the lower and upper limits are 2.2 and  $6.4 \text{ g} \cdot \text{cm}^{-3}$  because of the wide range in particle diameters. The grain density estimate was obtained from mass measurements on three samples of 100, 100, and 50 grains (selected from the 0.59- to 0.84-mm size bin). To avoid potential biases from counting out only large-size grains (and for confir-

| radionuclide      | $\gamma$ -ray energy<br>(keV) | NIST<br>calibration factor<br>for OS1 <sup>a</sup> | relative standard<br>uncertainty<br>(%) |
|-------------------|-------------------------------|--|---|
| <sup>241</sup> Am | 59.537                        | 0.005346   | 1.07                                    |
| <sup>109</sup> Cd | 88.0341                       | 0.013905   | 0.69                                    |
| <sup>57</sup> Co  | 122.0641                      | 0.019576   | 0.74                                    |
| <sup>139</sup> Ce | 165.857                       | 0.018256   | 0.58                                    |
| <sup>203</sup> Hg | 279.1967                      | [0.00484] <sup>b</sup>                             | [1.90]                                  |
| <sup>113</sup> Sn | 391.702                       | 0.00953  | 0.76                                    |
| <sup>85</sup> Sr  | 514.0076                      | 0.007149   | 0.74                                    |
| <sup>137</sup> Cs | 661.66                        | 0.006275   | 0.42                                    |
| <sup>88</sup> Y   | 898.042                       | 0.004295   | 0.57                                    |
| <sup>60</sup> Co  | 1173.238                      | 0.003502   | 0.39                                    |
| <sup>60</sup> Co  | 1332.502                      | 0.003151   | 0.39                                    |
| <sup>88</sup> Y   | 1836.063                      | 0.002409   | 0.59                                    |

<sup>a</sup> The calibration factor is the apparent "efficiency" given by the observed gamma-ray counting rates for each photon (as of 1200 EST, 1 October 1994) divided by their respective gravimetrically-determined  $\gamma$ -ray emission rates for the source (Table 1). The calibration factor does not include any corrections for source self-absorption or coincident-photon summing losses.

<sup>b</sup> This value for <sup>203</sup>Hg is not certified because of known spike losses.

Table 5. Calibration factors for standard OS1 as obtained with the NIST "T" detector.

mation), the determination was also made by weighing out about 100 mg of the sand and counting the total number of grains.

Based on the above average bulk density and grain density, the volume packing corresponds to roughly 64% of a maximum theoretical value ( $1.72/3.6 = 0.48$  compared to 0.741, since at closest packing 0.259 of the total volume is occupied by void spaces in a large volume of spheres of equal radii). Density of various silica minerals range from  $2.2 \text{ g} \cdot \text{cm}^{-3}$  to  $2.7 \text{ g} \cdot \text{cm}^{-3}$ . Using these as estimates of the grain density results in estimated volume packing of 106 and 86% of theoretical limits.

### Granular sodium chloride (GS)

This matrix was a USP/FCC granular NaCl, ob

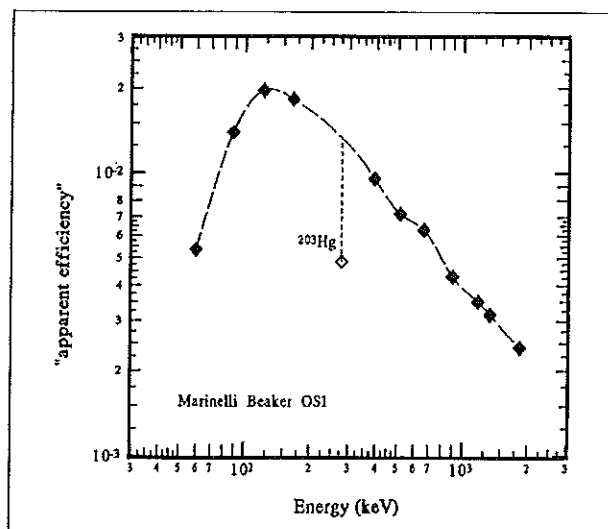


Figure 4. Calibration of the Marinelli-beaker calibration standard OS1 in terms of an apparent efficiency curve as obtained with the NIST "T" detector. The apparent efficiency includes source self-absorption and coincident-photon summing.

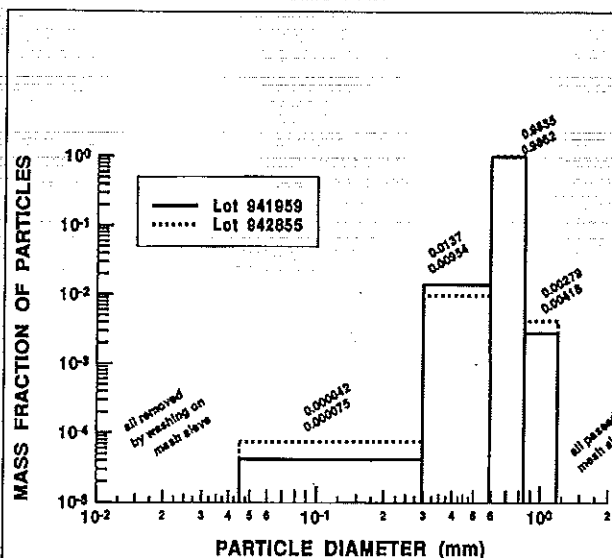


Figure A1. Particle-size distribution for Ottawa sand (two lots) in terms of the gravimetrically-determined mass fraction of particles versus particle diameter.

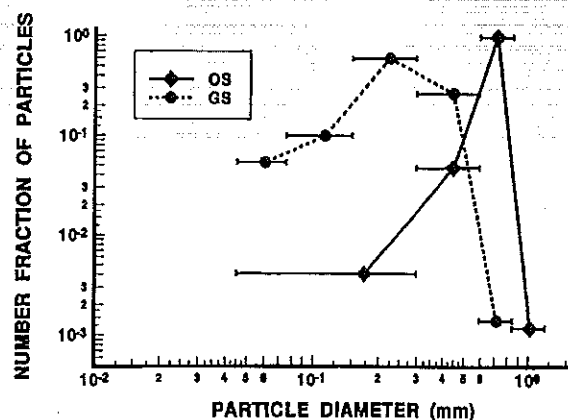


Figure A2. Particle-size distributions for Ottawa sand (OS) and granular NaCl (GS) in terms of the number fraction of particles versus particle diameter.

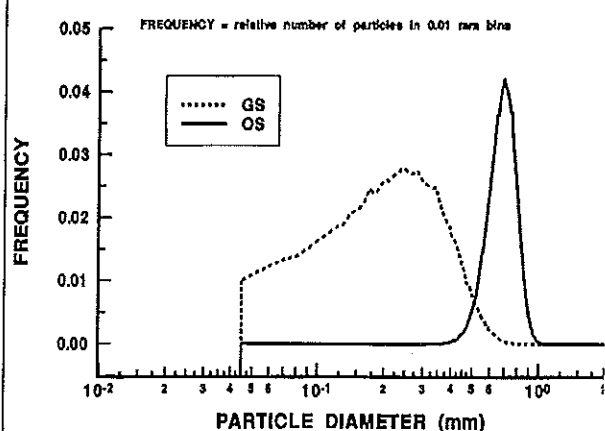


Figure A3. Fitted particle-size distributions for Ottawa sand (OS) and granular NaCl (GS), assuming truncated normal distributions for the particle diameters, to obtain derived mean diameters  $\mu$  and standard deviations  $\sigma$  for the distributions.

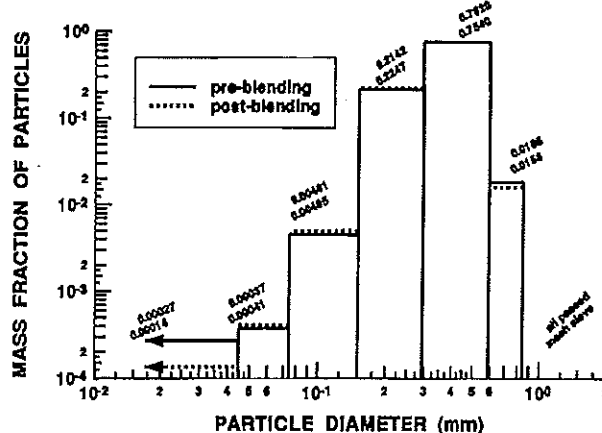


Figure A4. Particle-size distributions for granular NaCl (GS), for pre- and post-blending, in terms of the gravimetrically-determined mass fraction of particles versus particle diameter.

tained from Fisher Chemical. The bulk density was found to be  $1.36 \text{ g} \cdot \text{cm}^{-3} \pm 0.02 \text{ g} \cdot \text{cm}^{-3}$  where the cited uncertainty is a standard deviation with  $\nu=5$  degrees of freedom for 6 independent mass measurements in calibrated volumes of  $500 \text{ cm}^3$  and  $1000 \text{ cm}^3$ . As for the Ottawa sand, the density of GS depends on packing, but is also more variable because of the water content of the salt (extent of

drying).

The particle-size distribution may be characterized as  $0.26 \text{ mm} \pm 0.15 \text{ mm}$  (fitted parameters). Figures A4 (mass fractions), A2 (number fractions), and A3 (modeled distribution) give results treated comparably as that above for OS. As indicated, the particle sizes of GS compared to OS are smaller, and more broadly distributed. It was unknown

whether the salt would become finely pulverized during a blending process. Figure A4 gives the distributions before and after two hours of blending. There is no substantial difference in the two distributions indicating that powdering of the salt during blending is not a major concern.

Volume packing considerations for GS can be treated similarly to that given previously for OS. In this case, however, the known density of NaCl crystals can be used instead of an experimentally determined grain density. Assuming a NaCl grain density of  $2.17 \text{ g} \cdot \text{cm}^{-3}$ , the estimated volume packing is roughly 85% of the theoretical limit, that is comparable to that found for OS.

#### Disclaimer

Certain commercial equipment, instruments, or materials are identified in this paper to foster understanding. Such identification does not imply recommendation or endorsement by NIST, nor does it imply that the materials or equipment are necessarily the best available for the purpose.

#### Acknowledgments

The National Institute of Standards and Technology (NIST) is an agency of the Technology Administration of the U.S. Department of Commerce. Mr. F. Davis of the NIST Building and Fire Research Laboratory (Building Materials Division) is thanked for the loan of some apparatus used for the particle sizing; Ms. P.A. Hodge of the NIST Radioactivity Group is gratefully acknowledged for her meticulous counting of sand grains used to determine particle densities; Mr. J. Cessna, also of the NIST Radioactivity Group, is thanked for locating and assembling some of the necessary materials; and the efforts of Mr. R.D. Wampler (E. Byerly Co, Timonium, MD) in quickly securing a replacement laboratory blender for us (under severe deadlines) was deeply appreciated. This work was partially supported by funding through the Measurement Assurance Program for the Nuclear Power Industry,

a Cooperative Research and Development Agreement between the Nuclear Energy Institute and the NIST.

#### References

1. D.H. Gray, D.B. Golas, and J.M. Calhoun, "Review of the USCEA/NIST Measurement Assurance Program for the Nuclear Power Industry," *Radioact. Radiochem.*, **2**(1), 30-41, (1991).
2. R. Collé and F.J. Schima, "A Spiked, Mixed-Radionuclide, Mock "Soil" Marinelli-Beaker Calibration Standard for Gamma-Ray Spectrometry," unpublished progress reports (for the Nuclear Energy Institute, Steering Committee of the NEI/NIST Measurement Assurance Program for the Nuclear Power Industry), Radioactivity Group, National Institute of Standards and Technology (Sept., 1994 and Sept., 1995).
3. B.M. Coursey, "Use of NBS Mixed-Radionuclide Gamma-Ray Standards for Calibration of Ge(Li) Detectors used in the assay of environmental radioactivity," p. 173-179 in *Proceedings of a Symposium on Measurements for the Safe Use of Radiation*, S.P. Fivozinsky (ed.), National Bureau of Standards (NBS) Spec. Publ. 456, NBS, Wash., DC, 1976.
4. American National Standards Institute (ANSI) / Institute of Electrical and Electronic Engineers (IEEE), *Test Procedures for Germanium Gamma Ray Detectors*, ANSI/IEEE Standard 325-1986, ANSI, Philadelphia, 1986.
5. R.C. McFarland, "Coincidence Summing Considerations When Using Marinelli-Beaker Geometries In Germanium Gamma-Ray Spectroscopy," *Radioact. Radiochem.*, **2**(2), 4-7, (1991).

6. C.G. Sanderson and K.M. Decker, "A Mixed Gamma-Ray Standard for Calibrating Germanium Well Detectors," *Radioact. Radiochem.*, **4**(2), 36-41, (1993).
7. R.C. McFarland, "Effects of Nonuniformities in Soil Samples that are Gamma-Ray Counted in Marinelli Beakers," *Radioact. Radiochem.*, **3**(2), 6-10, (1992).
8. D.G. Olson and R.P. Bernabee, "Preparation and Analysis of High-Quality Spiked Soil Standards," *Health Physics*, **54**, 451-459, (1988).
9. C.W. Sill and F.D. Hindman, "Preparation and Testing of Standard Soils Containing Known Quantities of Radionuclides," *Anal. Chem.*, **46**, 113-118, (1974).
10. K. Debertin and R.G. Helmer, *Gamma- and X-Ray Spectrometry with Semiconductor Detectors*, North-Holland, Amsterdam, 1988, pp. 120-125 and 244-270.
11. K. Sinkko and H. Aaltonen, *Calculation of the True Coincidence Summing Correction for Different Sample Geometries in Gamma Ray Spectroscopy*, Finnish Centre for Radiation and Nuclear Safety, FCRNS Report STUK-B-Valo 40, Helsinki, 1985.
12. M. Clingan and W. Raines (Tennessee Valley Authority (TVA), Western Area Radiological Laboratory, Muscle Shoals, AL), private communications, July, 1994.
13. R. Collé, Zhichao Lin, F.J. Schima, P.A. Hodge, J.W.L. Thomas, J.M.R. Hutchinson, and B.M. Coursey, "Preparation and Calibration of Carrier-Free  $^{209}\text{Po}$  Solution Standards," *J. Res. Natl. Inst. Stds. Tech.*, **100**, 1-36, (1995).